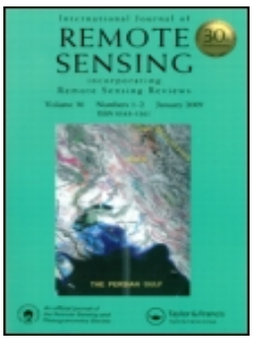

International Journal of Remote Sensing

ISSN: 0143-1161 (Print) 1366-5901 (Online) Journal homepage: https://www.tandfonline.com/loi/tres20

Power density of ocean surface wind from international scatterometer tandem missions

W. T. Liu , W. Tang , X. Xie , R. R. Navalgund & K. Xu

To cite this article: W. T. Liu , W. Tang , X. Xie , R. R. Navalgund & K. Xu (2008) Power density of ocean surface wind from international scatterometer tandem missions, International Journal of Remote Sensing, 29:21, 6109-6116, DOI: 10.1080/01431160802175439

To link to this article: https://doi.org/10.1080/01431160802175439

Published online: 23 Oct 2008.

International Journal of Remote Sensing
Vol. 29, No. 21, 10 November 2008, 6109–6116

Taylor & Francis
Taylor & Francis Group

Power density of ocean surface wind from international scatterometer tandem missions

W. T. LIU*†, W. TANG†, X. XIE†, R. R. NAVALGUND‡ and K. XU§
†Jet Propulsion Laboratory, California Institute of Technology, Pasadena, CA 91109, USA
‡Space Application Centre, Ahmedabad 38015, India
§Centre for Space Science and Applied Research, Chinese Academy of Sciences, Beijing, China

(*Received 29 April 2007; in final form 26 June 2007*)

For 6 months between April and October 2003, two identical scatterometers flew in tandem. Their observations demonstrate the need for more than one scatterometer in the polar orbit to include sufficient temporal variability and reduce aliasing of ocean surface wind-stress measurements required for applications such as estimating electricity generation potential and ocean–atmosphere gas exchange. The energy deficiency over a 12-h period, evident in the data from one scatterometer, is eliminated with the additional scatterometer. The missions in tandem allow an improved understanding of the diurnal variability from coastal regions to the open ocean. The power density distributions were found to be very different at the different sampling times of the two satellites. Two scatterometers will be launched by India and China in the next few years and will fly in tandem with the scatterometers of the USA and Europe, which are already in operation. The potential improvement in the coverage of ocean wind stress by this constellation is analysed and discussed. The constellation is found to meet the 6-hourly revisit requirement of operational weather forecasting over most of the ocean.

1. Introduction

A polar-orbiting scatterometer operating at a low altitude (e.g. 800 km) can sample at a location on Earth only two times a day. The temporal sampling may not be sufficient to monitor wind stress with high subdaily variability. An additional instrument flying in tandem should allow a description of higher temporal variability and a reduction in aliasing (bias introduced by subsampling) of the mean wind stress, as described by Lee and Liu (2005) in their study of the impact on ocean mixed layer depth. Liu and Xie (2006) have discussed the improved coverage of ocean surface wind by space-based sensors flying in tandem.

The radar scatterometer onboard the National Aeronautics and Space Administration (NASA) satellite QuikSCAT has provided global coverage of ocean surface wind-stress vectors and other terrestrial and cryospheric measurements since 1999 (Liu 2002). Data with improved spatial resolutions (12.5 km) have recently been produced and validated (e.g. Tang *et al*. 2004). A similar scatterometer was launched on the Japanese satellite Midori-2 in December 2002. This makes the construction of a diurnal cycle from coastal regions to open oceans possible (Liu and Tang 2007). In this paper, the older scatterometer onboard QuikSCAT is

International Journal of Remote Sensing
ISSN 0143-1161 print/ISSN 1366-5901 online
http://www.tandf.co.uk/journals
DOI: 10.1080/01431160802175439

referred to as QuikSCAT, and the newer scatterometer onboard Midori-2 is referred to as SeaWinds. Unfortunately, Midori-2 failed on 24 October 2003.

Liu (2003) described some potential applications opened up by the tandem missions. Both wind energy for electricity generation and surface gas flux depend on the third power of the wind speed; they are two examples examined using the data from the tandem missions. With the increasing demand for electric power and the need to reduce greenhouse gas emission, the demand to turn wind energy at sea into electric power has never been more evident. New technology has enabled floating wind-farms in the open seas to capture the higher wind energy and reduce the environmental impact on the coastal regions. Ocean–atmosphere exchange in greenhouse gases affects climate change and is also a timely concern. The gas exchange is highly dependent on wind speed (Wanninkhof and McGillis 1999, Carr *et al.* 2002), and significant variability in the carbon dioxide flux across the ocean surface has been observed, starting from the hourly frequency (Bates and Merlivat 2001). Although time series of wind from buoys at selected near-shore locations have been measured, spatial variability from coastal regions to open ocean has to rely on space-based sensors, and a constellation of sensors is needed to provide sufficient temporal coverage.

The data and the statistical analysis used in this work are described in section 2. Results from the tandem missions are presented in section 3. The potential of four scatterometers flying together and the expected sampling improvement are discussed in section 4.

2. Data processing

SeaWinds measurements were carefully calibrated to eliminate instrument bias and reprocessed with the same model function as QuikSCAT by the project engineers and science team. SeaWinds and QuikSCAT Level-2 (orbit-oriented format) data at 12.5 km resolution are obtained from the Physical Oceanography Data Active Archive Center (http://podaac.jpl.nasa.gov/). The scatterometer measurements, interpolated in space and time to the hourly buoy measurements, were used in the spectral analysis (figure 1). During the tandem mission period, from 10 April to 24 October 2003, there were roughly four measurements every day at the same location. When averaged over a period longer than 3 days, we were able to construct four wind-stress maps over the global ocean centred at local time of 06:00 (QuikSCAT, ascending), 10:30 (SeaWinds, descending), 18:00 (QuikSCAT, descending) and 22:30 (SeaWinds, ascending), all with complete spatial coverage. Using data available from the tandem mission period, we constructed four such time-series with 66 maps each, and also one time-series combining all data from QuikSCAT and SeaWinds. These maps are shown in figures 2 and 3. Hourly surface wind measurements were also obtained from the National Data Buoy Center (NDBC).

To assess the variability of wind at a particular location, a probability distribution function (pdf) was fit to the observed data. The Weibull distribution can be used to characterize the pdf of wind power (Pavia and O'Brien 1986, Barthelmie and Pryor 2003). A two-parameter Weibull distribution has the pdf (p) as a function of wind speed U:

$$p(U) = (k/c)(U/c)^{k-1} \exp\left[-(U/c)^k\right] \tag{1}$$

and the cumulative distribution function $P(U)$ is given by

$$P(U) = 1 - \exp\left[-(U/c)^k\right] \tag{2}$$

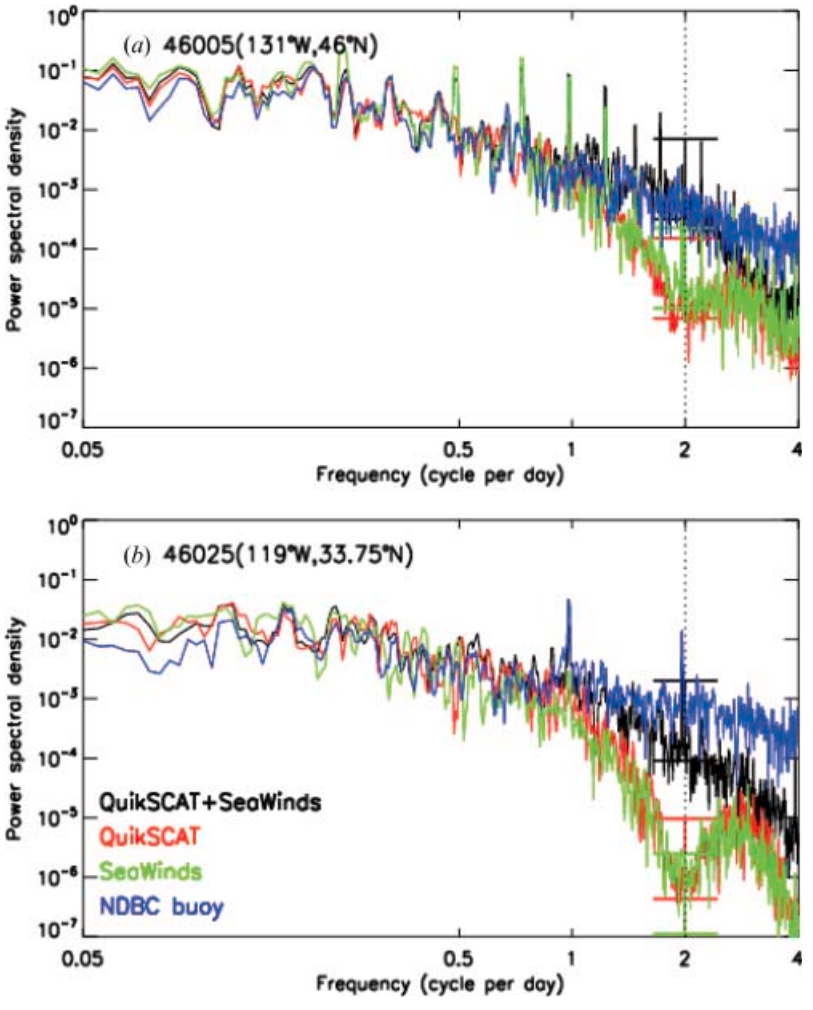

Figure 1. Power density spectrum calculated from collocated scatterometers and NDBC buoy data at (*a*) off-shore and (*b*) near-shore locations. Horizontal lines indicate 90% confidence intervals at semidaily frequency.

where k is a dimensionless shape parameter, and c is the scale parameter. A number of methods to estimate Weibull parameters exist, with negligible difference in the results (Monahan 2006). We used the simplest formula:

$$c = \bar{U}/\Gamma(1+1/k) \tag{3a}$$

$$k = \left(\bar{U}/\sigma\right)^{1.086} \tag{3b}$$

where $\bar{U}$ is the mean and σ the standard deviation of wind speed. The available wind power density E (which is proportional to U^3) can be calculated from the Weibull distribution parameters as

$$E = {}^1\!/_2\,\rho c^3\,\Gamma(1+3/k) \tag{4}$$

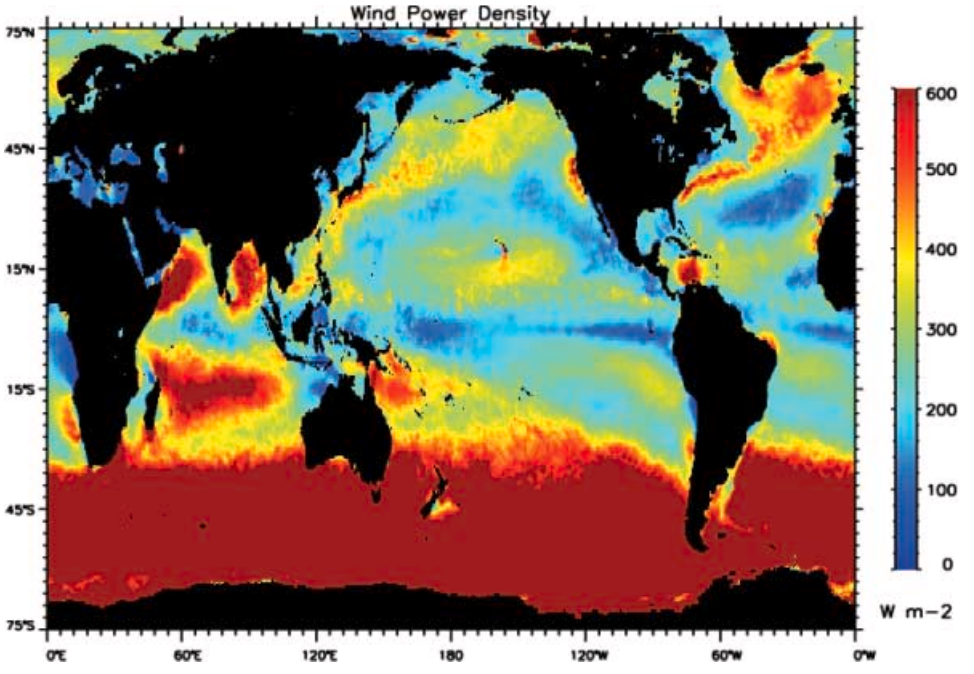

Figure 2. Wind power density estimated from ocean surface wind speed from tandem missions (QuikSCAT + SeaWinds).

where ρ is the air density and γ is the gamma function. The gas exchange coefficient should have similar characteristics.

3. Wind energy characteristics

When the wind from QuikSCAT or SeaWinds collocated with an offshore buoy was used, the power spectra (figure 1(*a*)) showed deficiencies at the semidaily frequency when compared with the spectra computed from wind measurement at the buoy alone. When the combined satellite data sets were used, the deficiencies were largely mitigated. Similar results were found at a near-shore location, as shown in figure 1(*b*), except that the deficiencies were much larger. For the semidaily frequency, the 90% confidence level of the spectrum for each individual scatterometer was separated from those of the combined data at both locations, inferring significant improvement by the tandem missions. The coastal region is strongly affected by a land–sea breeze (e.g. Gille *et al.* 2003). Two measurements a day are less likely to capture the diurnal cycle.

The wind power density E computed from combined QuikSCAT and SeaWinds data (figure 2) show the highest wind energy over the southern oceans, the 'Roaring Forties' and the 'Furious Fifties' around Antarctica. High energy is also found in the trade winds, the monsoon in the Indian Ocean, and the storm tracks in the North Pacific and North Atlantic. Low energy is found in the Equatorial Doldrums (Inter-Tropical Convergence Zone) and the Horse Latitudes. Similar patterns of E were observed separately from QuikSCAT or SeaWinds data and are therefore not shown. QuikSCAT shows higher E than SeaWinds on average, inferring that winds in the morning (06:00 h) and evening (18:00 h) have more energy than winds nearer to noon (10:30 h) and midnight (22:30 h). The data period, from April to October,

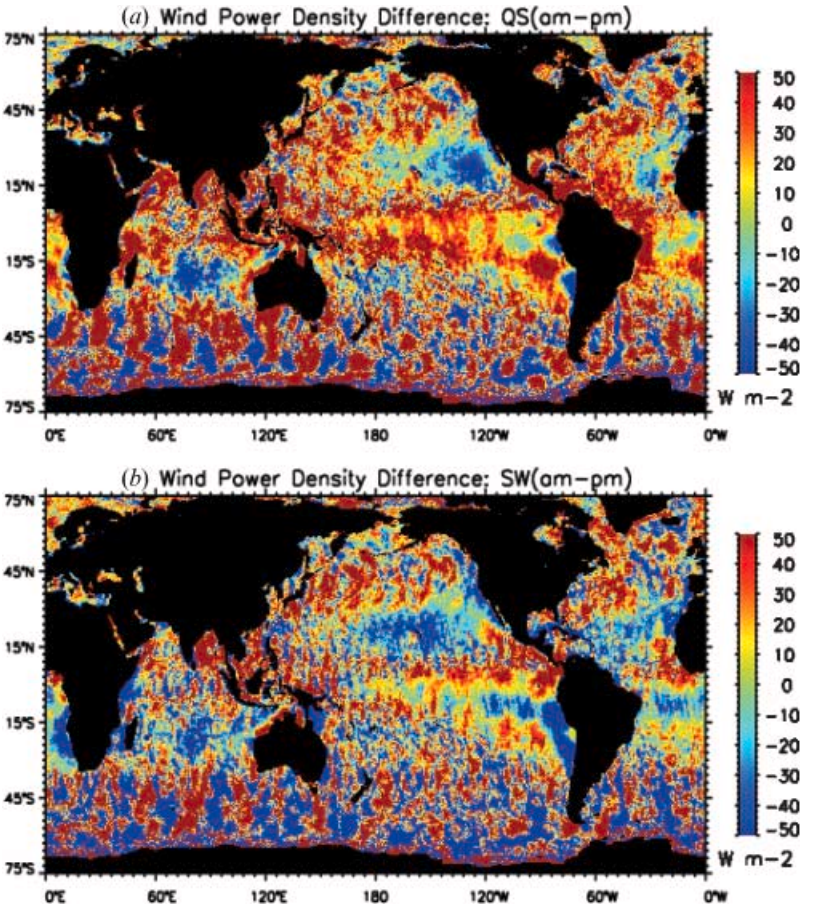

Figure 3. Diurnal differences in wind power density, as seen by (*a*) QuikSCAT and (*b*) SeaWinds (morning pass – evening pass).

covers the boreal summer, the Austral winter, and the strong summer monsoon in the Indian Ocean. The distributions of carbon dioxide flux (not shown) have similar geographic distribution and temporal dependence.

Figure 3 shows that the difference in E between morning and evening passes for QuikSCAT and SeaWinds. The major patterns are similar. In the tropical oceans and mid-latitude North Pacific and Atlantic Oceans, the energy is higher in the morning than the evening. In the subtropical oceans, particularly the eastern parts, there is more energy in the evening than in the morning.

4. Present and future mission coverage

After the failure of Midori-2 in October 2003, there was only one scatterometer in operation until the launch of the Advanced Scatterometer (ASCAT) on the European Meteorology Operational Platform (METOP) in October 2006. The Indian Oceansat-II and the Chinese Haiyang-2 satellites are planned to be launched in 2008 and 2010, respectively, each with a scatterometer on board. Table 1 shows the major parameters of the four present and near future scatterometer missions. The equatorial crossing times of Haiyang-2 are almost the same as QuikSCAT, but

Table 1. Platform and sensor parameters of four scatterometer missions.

	Orbit inclination (deg)	Orbit period (min)	Swath width (km)	LTAN	Orbit height (km)
QuikSCAT	98.7	101.05	1900	05:54	803
ASCAT	98.7	101.35	1100	21:30	817
Oceansat-II	98.3	99.30	1840	12:00	720
Haiyang-2	99.0	124.83	1700	18:00	965

LTAN, local time of ascending node.

those of ASCAT and Oceansat-II are different and would complement each other in sampling the daily variability. ASCAT is a fan-beam scatterometer with two 550-km swaths separated by a nadir gap, measuring at C-band. The designs of Oceansat-II and Haiyang-2 are similar to QuikSCAT. Both are ku-band, pencil-beam, conically scanning scatterometers, with horizontal polarization for the inner beam and vertical polarization for the outer beam. The swath width given in table 1 is for the outer beams. With an ocean colour sensor onboard, Oceansat-II chose a lower orbit height and will have a shorter orbiting period and a higher incident angle than QuikSCAT. Haiyang-2 will fly with a radar altimeter at a higher orbit with a longer orbiting period and lower incident angle. The equatorial crossing time for Haiyang-2 may be either for the ascending or the descending orbit.

As shown in figure 4, ASCAT has the lowest coverage because of the swath width; it takes 2 days to cover 90% of the Earth. Haiyang-2 has a longer period and will cover 90% of the Earth in 36 h. Indian Oceansat-II will fly in a slightly lower orbit, will have slightly narrower swath, and will provide similar coverage to QuikSCAT; either QuikSCAT or Oceansat-II will cover 90% of the Earth in 24 h. The

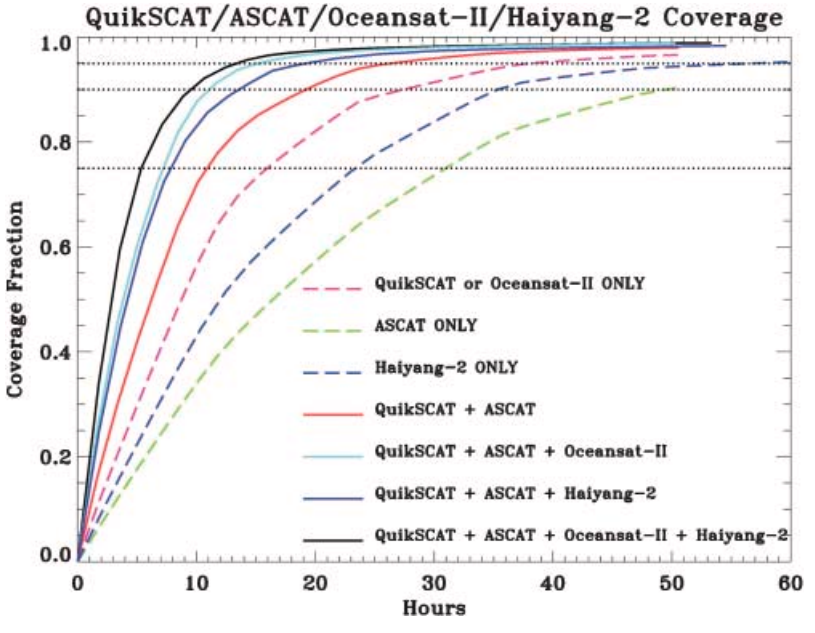

Figure 4. Fractional coverage of the Earth, between 70° N and 70° S, as a function of time, for various tandem missions.

combination of QuikSCAT and ASCAT will cover 90% of the Earth in 18 h. Adding either Haiyang-2 or Oceansat-II, we will be able to achieve 90% coverage in less than 12 h. In every 6 h, the constellation will cover 85% of the Earth.

Since the orbits come closer at high latitudes, the zonally averaged revisit interval decreases from the equator towards the poles. As shown in figure 5, the interval decreases from 28 h at the equator to 9 h for ASCAT, and from 17 h to 5 h for QuikSCAT. The constellation will provide less than a 6-hourly revisit interval for all latitudes, meeting operational weather forecast requirements.

5. Discussion

The 6 months of observations by two identical scatterometers flying in tandem demonstrate that more than one polar-orbiting instrument is needed to include the high frequency variability and to reduce the aliasing introduced by undersampling. Generating electric power and deriving ocean–atmosphere exchanges in carbon dioxide were the two examples shown to require such high temporal resolution.

High-frequency wind fields can be obtained using satellites in low Earth orbits (e.g. 800 km), either with a constellation of instruments in polar orbits or with a single instrument in a low-inclination orbit. An instrument in a low inclination orbit will not cover the mid- and high-latitude oceans. High frequency can also be achieved by flying a scatterometer at a high altitude, which optimizes the swath width, but below the hostile radiation environment (e.g. 1500 km). Spatial resolution may be compromised or a technologically challenged large antenna is needed at such a high altitude.

Even the combination of QuikSCAT and SeaWinds would not provide a 6-hourly revisit time over most of the non-polar oceans. An international constellation of scatterometers in a low-altitude polar orbit is the most promising. Deriving a consistent merged product may need international cooperation in calibration, and

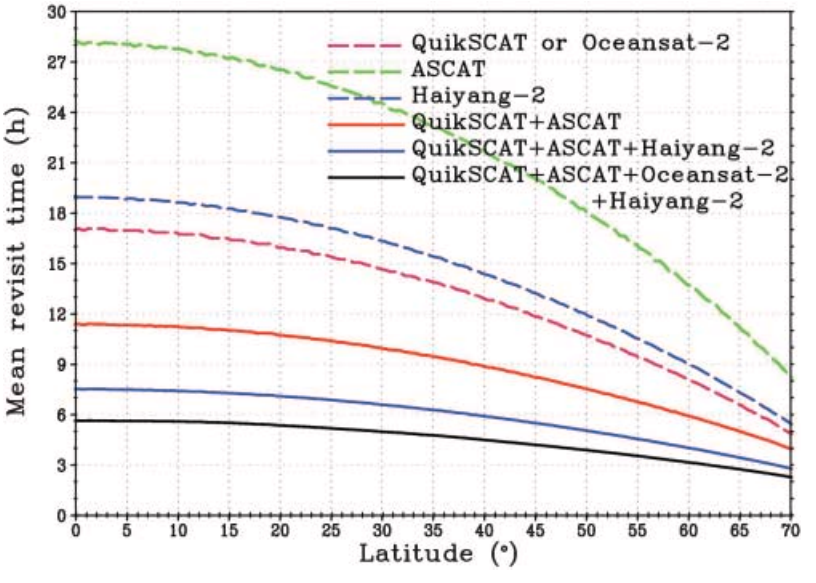

Figure 5. The latitudinal variation of zonally averaged revisit intervals for various tandem missions.

maintaining the product over time may require political will and international support.

Acknowledgements

This study was performed at the Jet Propulsion Laboratory, California Institute of Technology, under contract of the National Aeronautics and Space Administration (NASA). W.T.L., W.T. and X.X. were supported by the Physical Oceanography and Ocean Vector Wind Programs of NASA.

References

BARTHELMIE, R.J. and PRYOR, S.C., 2003, Can satellite sampling of offshore wind speeds realistically represent wind speed distributions? *Journal of Applied Meteorology*, **42**, pp. 83–94.

BATES, N.R. and MERLIVAT, L., 2001, The influence of short-term wind variability on air–sea CO_2 exchange. *Geophysical Research Letters*, **28**, pp. 3281–3284.

CARR, M.E., TANG, W. and LIU, W.T., 2002, CO_2 exchange coefficients from remotely sensed wind speed measurements: SSM/I versus QuikSCAT in 2000. *Geophysical Research Letters*, **29**, pp. 30.1–30.4.

GILLE, S.T., SMITH, S.G.L. and LEE, S.M., 2003, Measuring the sea breeze from QuikSCAT scatterometry. *Geophysical Research Letters*, **30**, pp. 14.1–14.4.

LEE, T. and LIU, W.T., 2005, Effects of high-frequency wind sampling on simulated mixed layer depth and upper ocean temperature. *Journal of Geophysical Research*, **110**, pp. C05002.1–C05002.9.

LIU, W.T., 2002, Progress in scatterometer application. *Journal of Oceanography*, **58**, pp. 121–136.

LIU, W.T., 2003, *Scientific Opportunity Provided by SeaWinds in Tandem*, JPL Publications 03-12 (Pasadena: Jet Propulsion Laboratory).

LIU, W.T. and TANG, W., 2007, Diurnal cycle of ocean surface wind-stress observed by two scatterometers. *Geophysical Research Letters*, submitted.

LIU, W.T. and XIE, X., 2006, Measuring ocean surface wind from space. In *Remote Sensing of the Marine Environment: Manual of Remote Sensing*, Bethesda, MD, 3rd edn, Vol. 6, J. Gower (Ed.), pp. 149–178 (The American Society for Photogrammetry and Remote Sensing).

MONAHAN, A.H., 2006, The probability distribution of sea surface wind speeds. Part I: Theory and SeaWinds observations. *Journal of Climate*, **19**, pp. 497–520.

PAVIA, E.G. and O'BRIEN, J.J., 1986, Weibull statistics of wind speed over the ocean. *Journal of Climate and Applied Meteorology*, **25**, pp. 1324–1332.

TANG, W., LIU, W.T. and STILES, B.W., 2004, Evaluation of high-resolution ocean surface vector winds measured by QuikSCAT scatterometer in coastal region. *IEEE Transactions on Geoscience and Remote Sensing*, **42**, pp. 1762–1769.

WANNINKHOF, R. and MCGILLIS, W.R., 1999, A cubic relationship between air–sea CO_2 exchange and wind speed. *Geophysical Research Letters*, **26**, pp. 1889–1892.